P1.5

COMPARING CONVECTIVE WEATHER AVOIDANCE MODELS AND AIRCRAFT-BASED DATA*

Rich DeLaura†
Brad Crowe
Richard Ferris
Massachusetts Institute of Technology, Lincoln Laboratory
244 Wood Street
Lexington, MA 02420

John F. Love
William N. Chan
NASA Ames Research Center
Moffett Field, CA 94035

1. INTRODUCTION

The Convective Weather Avoidance Model (CWAM), developed in collaboration with NASA, translates convective weather information into a Weather Avoidance Field (WAF), to determine if pilots will route around convective regions. The WAF provides an estimate of the probability of pilot deviation around convective weather in en route airspace as a function of time, horizontal location, and flight altitude [1][2]. The results of the WAF can used to create reroutes around regions of convective weather where pilots are more likely to deviate. If reliable WAF information is provided to the cockpit and ground, pilot decisions may become more predictable, simplifying the task of air traffic control in convective weather.

The improvement and validation of CWAM requires inference of pilot intent from flight trajectory data, which is challenging. The process currently involves laborious human review of the results of automated deviation detection algorithms. Both previous CWAM studies and a recent validation study [3] illustrate the difficulties and limitations of attempting to infer pilot intent from flight trajectory data. Furthermore, observed flight tracks may not correctly represent pilot preference. In some instances, pilots may have penetrated airspace that they would rather have avoided or they may have avoided airspace that was easily passable.

In order to improve and assess the accuracy of the WAF, it is desirable to compare WAF predictions of pilot intent with direct evidence of the airborne experience during weather encounters in en route airspace, such as normal acceleration. To achieve this, a series of flights using a research aircraft was conducted. In the summer of 2008, four research flights (three on 17 July and one on 14 August) were flown in and around convective activity in the upper Midwestern United States to gather aircraft data that could be correlated to the WAF and other remotely-sensed weather data. The aircraft, a Rockwell Sabreliner Model 50 research aircraft (similar to the Sabreliner Model 40 production model) owned by Rockwell-Collins, flew through and around convective activity while recording on-board accelerations for comparison to the WAF deviation probabilities encountered along the flight trajectory. Aircraft state data, on-board weather radar images, video, photographs and pilot narrative from the cockpit were also collected.

This paper briefly describes the CWAM model and WAF. Description of the data collection methodology is then presented. Following that section are descriptions of the flights comparing radar data from the flight deck with ground-based weather radar and the WAF. Visual observations and pilot narrative from the flight deck are also presented. Next, the normal acceleration data from on-board accelerometer data are compared with WAF. Finally, conclusions and suggestions for further study are presented.

2. BACKGROUND

Aviation weather systems such as the Corridor Integrated Weather System (CIWS) [(Klingle-Wilson and Evans, 2005) provide weather information and forecasts that aid en route traffic managers in making tactical routing decisions to mitigate the impact of convective weather.

*This work was sponsored by the National Aeronautics and Space Administration (NASA) under Air Force Contract FA8721-05-C-0002. Opinions, interpretations, conclusions, and recommendations are those of the authors and are not necessarily endorsed by the United States Government.

†*Corresponding author address*: Rich DeLaura, MIT Lincoln Laboratory, 244 Wood Street, Lexington, MA 02420-9185; e-mail: richd@ll.mit.edu

Rerouting advisory algorithms can be developed for automated ATM decision support tools to take advantage of weather systems like CIWS. These advisories must be acceptable to the pilots who are expected to fly them with minimal revision. Automated advisories that require several iterations before acceptance will increase the workload on the pilot and controller reducing the overall usefulness of these advisories.

CWAM translates convective weather information from CIWS into impact on aircraft by determining which convective regions pilots will choose to avoid. Understanding pilot preference for deviation can then be used to create weather-reroutes, which then can be used to estimate a reduction in capacity of airspace. CWAM creates a Weather Avoidance Field (WAF), which estimates the probability between 0 – 1.0 (0 to 100%) of pilot deviation around convective weather in en route airspace as a function of time, location and flight altitude. High WAF probabilities indicate areas where pilots are more likely to deviate.

In this study, the WAF from two different versions of the CWAM (DeLaura and Evans, 2006 and DeLaura et. al., 2008) are evaluated. In CWAM 1, WAF deviation probabilities are a function of the difference between flight altitude and convective height and convective intensity for specific spatial coverage. Convective height is defined by the 18 dBZ echo top and intensity is defined by Vertically Integrated Liquid (VIL). The height used at a particular pixel is the 90th percentile echo top in a 16 x 16 km box centered on the pixel, and VIL intensity is calculated as the percentage of VIL pixels >= VIP level 3 over a 60 x 60 km box. In CWAM 2, WAF deviation probability is a function of the difference between flight altitude and convective activity height, and the spatial coverage of echo tops >= 30kft over a 16 x 16 km box centered on the pixel. As a result of the spatial filtering (figure 1), WAF tend to be smoother than the observed weather (figure 2) and create buffers around intense convective cells.

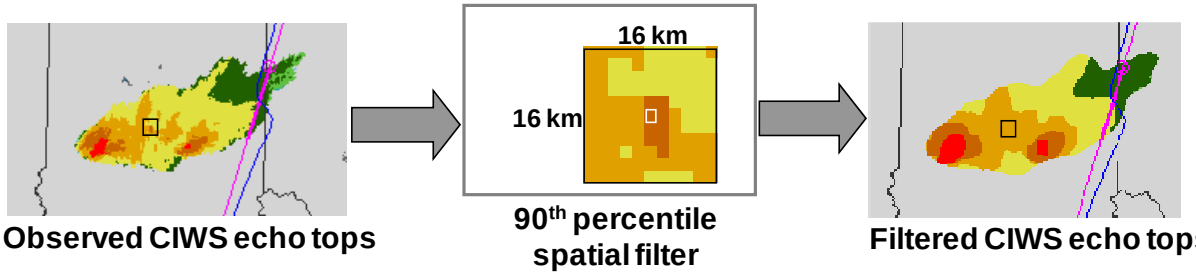

Figure 1. Spatial filtering of weather fields for incorporation in convective weather avoidance models (CWAM).

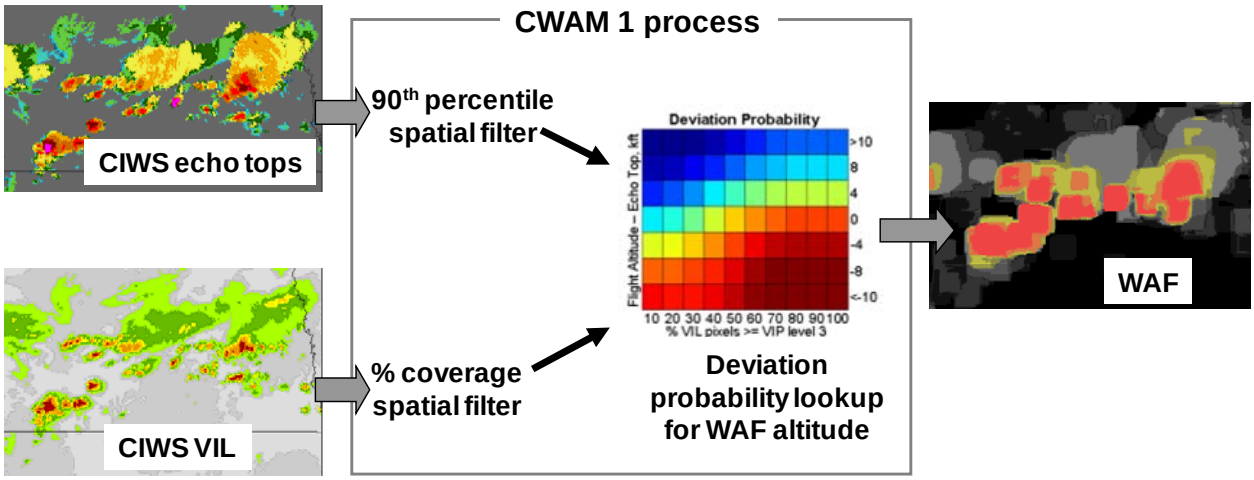

Figure 2. Generation of weather avoidance fields (WAF) using CWAM 1.

Another method to develop a convective weather translation model confirmed the results of previous CWAM studies. It identified the difference between flight altitude and echo top height as the primary predictor of pilot deviation in en route airspace, and it required less human intervention. This weather translation model (Kuhn, 2008) used an alternative statistical method to infer pilot intent. By cross-correlating aircraft occupancy with weather occupancy of grid volumes, the method eliminates the need to validate the classification of individual flight trajectories, thereby greatly reducing the labor involved in the analysis. Unfortunately, many weather conditions were associated with deviation probabilities between 0.3 and 0.7, which makes it difficult to decide if a pilot will deviate to avoid weather.

Both of these models need to be validated, but previous validation of the CWAM has shown to be time consuming. It is difficult to identify and validate, despite the use of automation, weather-avoiding deviations. Deviation detection algorithms used in the CWAM studies have error rates estimated to be around 30% (DeLaura and Evans, 2006; DeLaura et. al., 2008). Human evaluation of each classification, deviating or not deviating, was required to ensure the validity of the data set.

A more direct method to improve and evaluate the accuracy of pilot decision making that could improve the CWAM or other similar models is to analyze the experience on the flight deck, where the deviation decisions are made. There should be a positive correlation between high WAF values and cockpit cues (turbulence, visual sighting of convective towers or anvils, indication of weather hazards on airborne weather radar, etc) that result in pilot decisions to deviate. It is important to understand the relationship between remotely-sensed data that contribute to the WAF and the information available to the pilot. Potential improvements to the CWAM may be revealed by examining the convective regions where pilot behavior is predicted poorly and identifying the information pilots use to make routing decisions in those circumstances.

3. METHOD

A comparison was made between WAF probabilities and aircraft information for several flights; a comprehensive statistical validation requires more data than were collected for this study. CWAM 1 and 2 WAFs were calculated using observed CIWS VIL and echo tops as inputs for the predominant mission flight altitude (34kft) over the regions of each flight. These data were then compared to data recorded from the instrumentation aboard the Rockwell Collins research aircraft. The research aircraft was equipped with a fixed, forward-looking video camera, cockpit audio recorder, photographer, Inertial Navigation System (INS), global positioning system (GPS), an XM WX Satellite Weather® data display from XM Satellite Radio Inc., and a Rockwell Collins airborne weather radar (model WXR2100) that is currently installed in a wide range of commercial aircraft. Video and audio data were time stamped. INS data included position, airspeed and accelerations along x, y, z, normal, roll, pitch and yaw axes and wind speed and direction. GPS data included position and altitude. Temperature, pressure and altimeter altitude were also recorded.

All flight data were recorded at 50 Hz. Cockpit weather radar images were recorded continuously as the radar display updated. The cockpit weather radar was set to maintain a radar zenith angle of approximately -2.25 degrees down from the horizontal plane. This is a common practice among commercial pilots who wish to identify intense reflectivity below flight level that has potential for rapid growth [personal communication, Rockwell Collins engineering team]. Figure 3 shows the cockpit instrumentation. The WAF was calculated every 2.5 minutes in synchrony with the CIWS VIL and echo top mosaic updates.

Time series of the WAF probabilities encountered at each second along the flight trajectories were generated by extracting values at the nearest neighbor grid point. These time series were compared to the time series of normal acceleration recorded from the aircraft's INS. The aircraft location was plotted over observed weather and WAF to determine the aircraft location relative to the convective storm. Wind measurements from the aircraft were used to determine whether the aircraft was upwind or downwind from convective cells. Cockpit weather radar images were synchronized with aircraft location data to examine the correlation between airborne and ground radars. Video and cockpit photos were used to determine when thunderstorms were visible from the cockpit, and pilot narrative provided additional information about factors that affect pilot decision making. The analysis also includes a description of the weather and commercial air traffic conditions at the time of the flight mission.

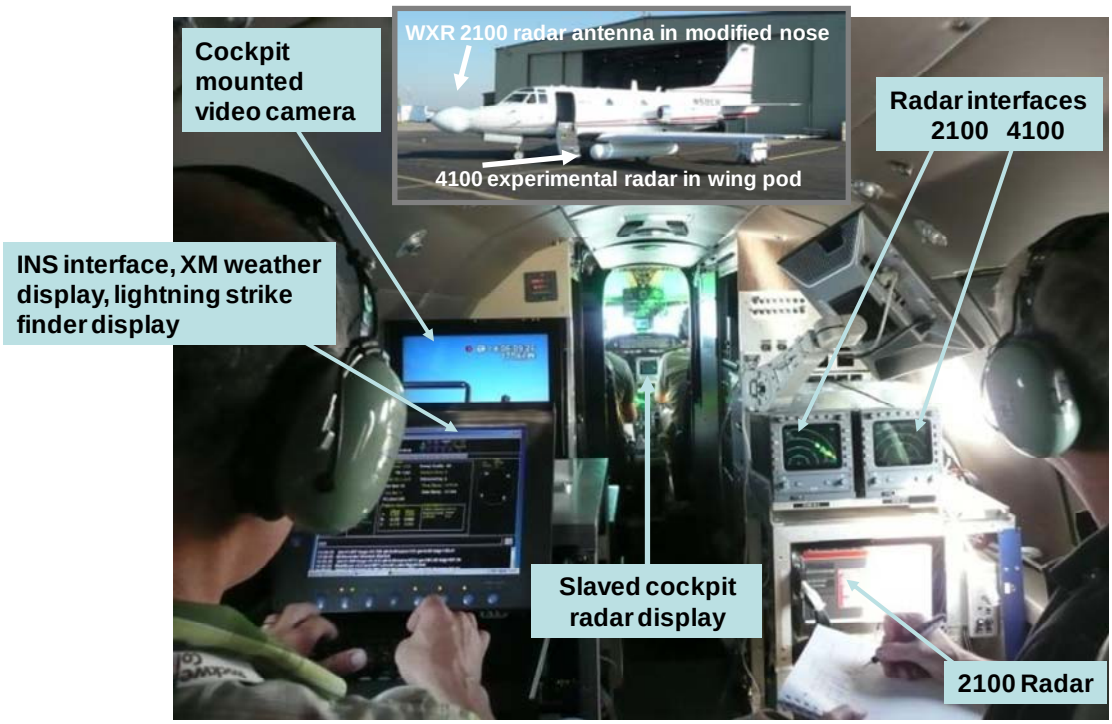

Figure 3. Photo of the research aircraft interior.

References to the severity of turbulence follow the criteria established by the World Meteorological Organization. Normal accelerations between 0.5 and 1.0 g are described as moderate turbulence; accelerations between 0.15 and 0.5 g are considered light turbulence. According to the International Civil Aviation Organization, in moderate turbulence, walking is difficult and passengers feel definite strains on their lap belts (Lester, 1993). The aircraft never encountered normal accelerations greater than 0.8 g (moderate turbulence) during the flight missions.

This study focused on mesoscale and 'popcorn' convection, which present challenges to both forecasters and pilots. Data were gathered from several areas of interest within convective storms: the leading (growing) edge and cores of convective cells, the decaying region behind mature convective cells and downwind thunderstorm anvils (figure 4).

Ground control at Lincoln Lab directed the flights into regions of interest based on the real-time monitoring of aircraft locations via the ETMS research feed, VIL, and echo tops measurements from CIWS. The aircraft crew, including the research pilot, radar engineers from Rockwell Collins and a researcher from Lincoln Lab, refined the direction of ground control as needed to capture the most interesting areas of convective activity and to avoid hazards.

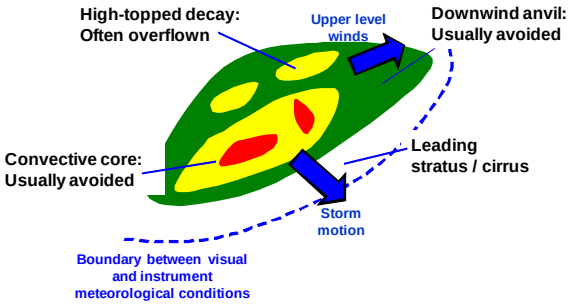

Figure 4. Regions of interest in and around convective storms.

4. FLIGHT DESCRIPTIONS

4.1 Day 1: 17 July, 2008

Three research flights were flown in the presence of an old, slow moving frontal boundary, stretched from Colorado and Nebraska into Minnesota. The boundary sagged south and east during the day and had a history of producing clusters of thunderstorms, some of which persisted throughout the day and into the night in the form of mesoscale convective complexes. Some thunderstorms were enhanced and became severe during the afternoon as a consequence of short waves moving through the primarily west to east upper level flow.

The first flight, which flew from approximately 1430Z – 1630Z, departed from Cedar Rapids Iowa (CID) into the southern half of Minnesota, with return to Iowa and landing in Sioux Falls, South Dakota. A large area of level 3-6 thunderstorms was present in southern Minnesota with echo tops up to 50kft. Few commercial aircraft were observed in the vicinity of the storm. However, steady streams of commercial traffic were observed well north (downwind) of the convective line and rounding the upwind edge of the cells to the southwest. Figure 5 illustrates the flight track overlaid on observed VIL and echo tops, a Flight Explorer image showing all commercial traffic flying at altitudes greater than or equal to 18kft., and the downsampled time history of normal acceleration recorded from the aircraft's INS. Although the flight track depicts an approximately 1.5 hour flight, only one representative weather radar image shapshot is shown. The purple circle on the flight explorer weather radar image coincides with the aircraft position along the flight track. Note that the weather depicted in the Flight Explorer image is composite reflectivity, which presents details of some convective regions differently from the CIWS VIL product.

The flight initially penetrated a growing convective line embedded in a large region of stratiform rain at around 1430z (figure 5, pointer A). The line was approached from the downwind, leading edge in instrument meteorological conditions (IMC). The aircraft encountered level 5 VIL with echo tops between 35 and 40kft in the convective core. The onset of turbulence was felt 2-3 minutes before the entrance into the convective core, while the aircraft was flying through level 1 VIL and 35 – 40kft echo tops downwind of the core. WAF deviation probabilities ranged between 0.60 and 0.80 throughout the encounter. Measured normal acceleration ranged from approximately 0.1 to 0.3 g (light to moderate turbulence).

The onboard weather radar generally agreed with ground-based radar, showing high reflectivity regions and turbulence detections from an experimental on board algorithm that aligned well with high probabilities of deviation in the WAF. However, as the aircraft drew closer to the storm, reflectivity decreased on the on board radar display and a gap appeared to open in the middle of the line (figure 6). This may have resulted from decreased beam filling as the aircraft approached the storm core. At longer ranges, the radar beam samples a wider range of altitudes and senses a large portion of lower altitude, high reflectivity storm cores. At shorter ranges, the beam volume of the aircraft weather radar spans a smaller range of higher altitudes only, and misses high reflectivity storm cores below.

The XM weather display (not shown) also suggested severe weather, showing all red cells (50 dBZ or greater) and tops in the 50 kft. range. The pilot noted that he would expect commercial pilots to deviate: "…if you're asking, I would not fly through this. Why beat up your airplane when you can make a clear cut left turn [into a region where both on board radar and XM showed clear air]?" However, upon passing through the weather, the pilot noted that the turbulence experienced was less than anticipated.

After passing through the convective line, the flight continued in IMC through a region of decaying stratiform rain characterized by level 2 – 3 VIL and echo tops ranging from 30 – 35kft. WAF in this region decreased from approximately 0.7 to 0.2, as the distance from the convective line increased, and there was little or no turbulence, with measured normal accelerations < 0.1 g (figure 5, pointer B).

After a third right turn, the aircraft then maneuvered north of the convection to position itself to pass the line on the eastern edge of the system (downwind of the strongest region of convection). Then the aircraft entered an area of light to moderate turbulence (persistent normal accelerations ranging between 0.2 and 0.3 g) downwind from active convection. WAF values for this same region ranged from 0.2 to 0.3 (figure 5, pointer C and figure 7). Figure 7 shows turbulence increased as the flight approached stronger cells at the growing edge of the line. The winds at flight level were fairly strong throughout this phase of the flight, approximately 60 knots. At this point, the pilot stated that he would ordinarily avoid this downwind region, turning away to stay a greater distance from the visually observed anvil. Eventually, the aircraft cleared the downwind turbulence, far downwind of the leading edge of the storm. Throughout this phase of the flight, the onboard radar showed generally good agreement with ground-based radar.

The region of transition between stratiform rain on the decaying edge of the line and more turbulent downwind anvil was not clearly evident from either the ground radar (and the WAF derived from it) or the airborne radar. Turbulence was encountered approximately 30 nautical miles downwind of vigorous convection, characterized by level 5 - 6 precipitation intensity and echo tops up to 50 kft. While the onset of turbulence was readily evident in the INS acceleration data, defining the boundary of the turbulent region

precisely from ground-based radar and wind observations is difficult due to the relatively low spatial resolution and temporal update rate of the ground based radar and wind estimation models.

The aircraft made a second approach to the growing convective line from the downwind leading edge. Heading into a level 6 VIL and 50kft cell the pilot eventually turned back due to increasing turbulence (peak normal acceleration of 0.7 g, corresponding to moderate turbulence). WAF deviation probabilities ranged between 0.70 and 0.90 (figure 5, pointer D). The onboard weather radar detected turbulence in the region and showed high reflectivity features that corresponded with the strong convective regions that were evident on ground based radar. The aircraft encountered no hail but did fly into significant amounts of graupel.

Flight 2 flew from approximately 1900Z – 2100Z from Sioux Falls SD, across Nebraska to Denver Colorado, and back to North Platte, Nebraska for a refueling stop (figure 8). This second flight penetrated a large level 6 VIL and 50kft cell in eastern Nebraska (figure 8, pointer A and figure 9). In this instance, winds were approximately perpendicular to the direction of flight. As a result, the aircraft flew from smooth and clear (IMC) air almost directly into the core, approaching from the trailing edge, moving very rapidly from level 2 to level 6 VIL and back to smooth and clear air as it emerged through the leading edge of the cell. Turbulence was moderate (peak normal accelerations of 0.6 g). The WAF probabilities ranged between 0.80 to 1.0. Note that the WAF provides a buffer along the high-gradient edges of the cell.

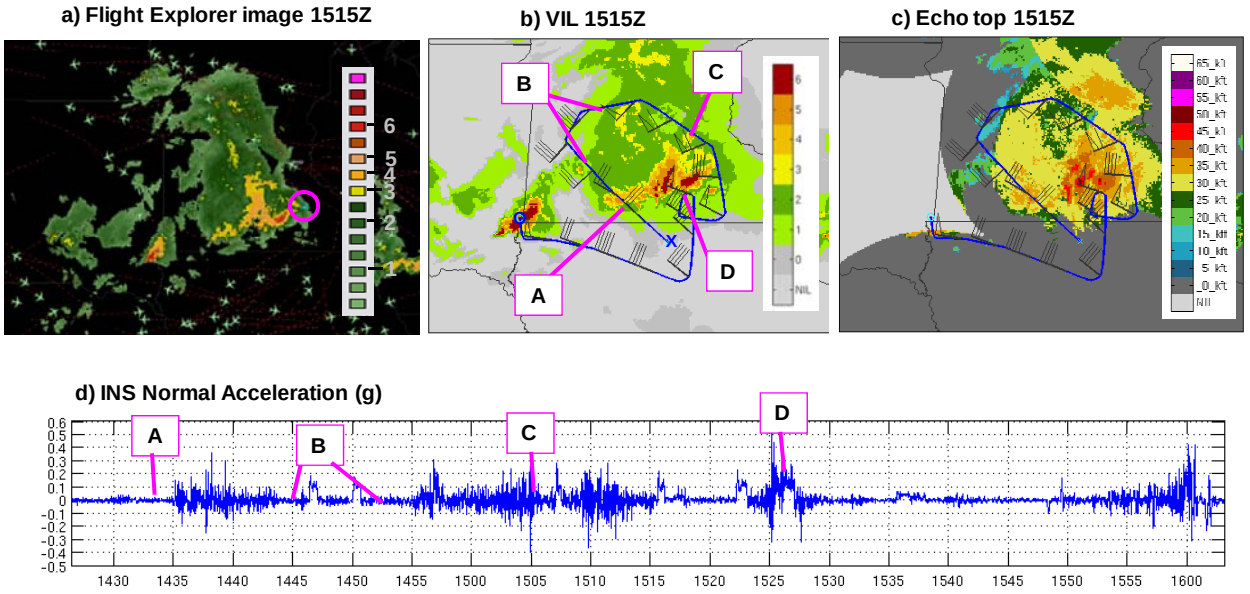

Figure 5. Summary of flight #1 on 17 July, 2007. Flight Explorer image showing research aircraft (magenta circle), (a) composite reflectivity (accompanying color scale shows Video Integrated Processor (VIP) levels that correspond to CIWS VIL color scale) and nearby commercial traffic at altitudes >= 18kft , (b) flight track overlaid on CIWS VIL ('X' marks the start of the flight, (c) 'O' marks the end), (d) echo tops, and normal acceleration recorded from the aircraft's Inertial Navigation System (INS). Pointers identify regions described in section 4.1.

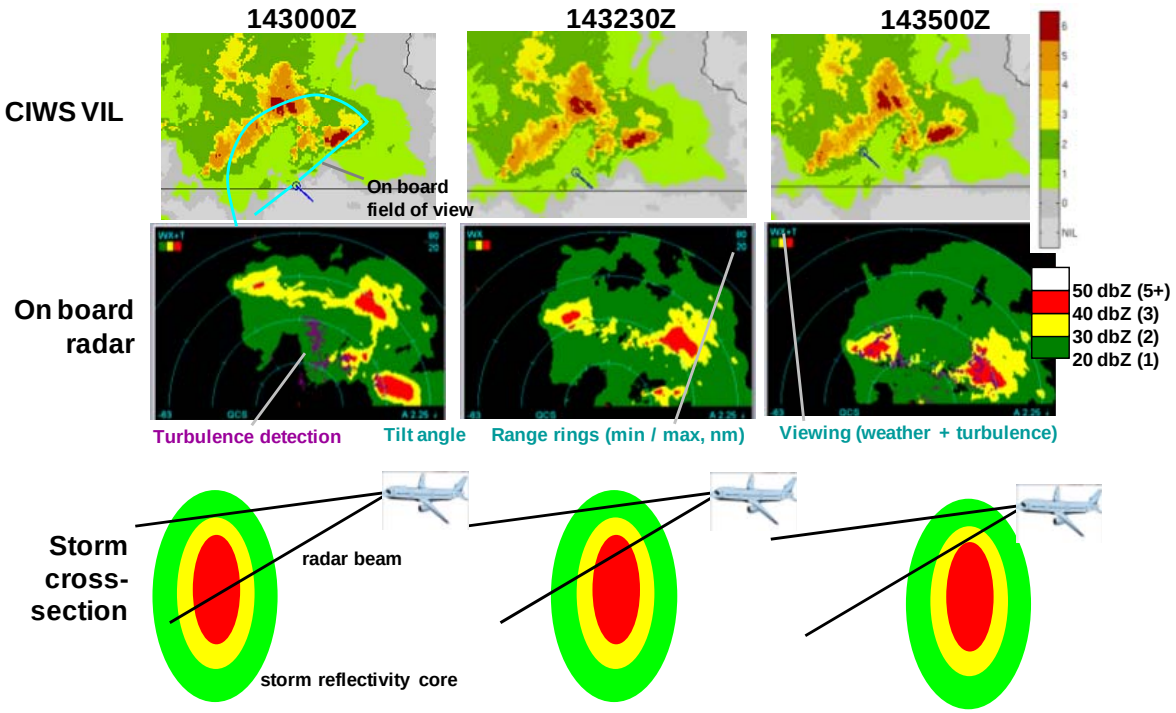

Figure 6. Comparison of ground and airborne weather radar images. Top row shows aircraft location overlaid on CIWS VIL map. Middle row shows on board radar display with arrows pointing towards descriptions of data and mode. Purple regions on weather radar view depict turbulence identified by the on board radar turbulence detection algorithm. Bottom row shows the issue of reduced filling of on board weather radar beam as aircraft approached convective core.

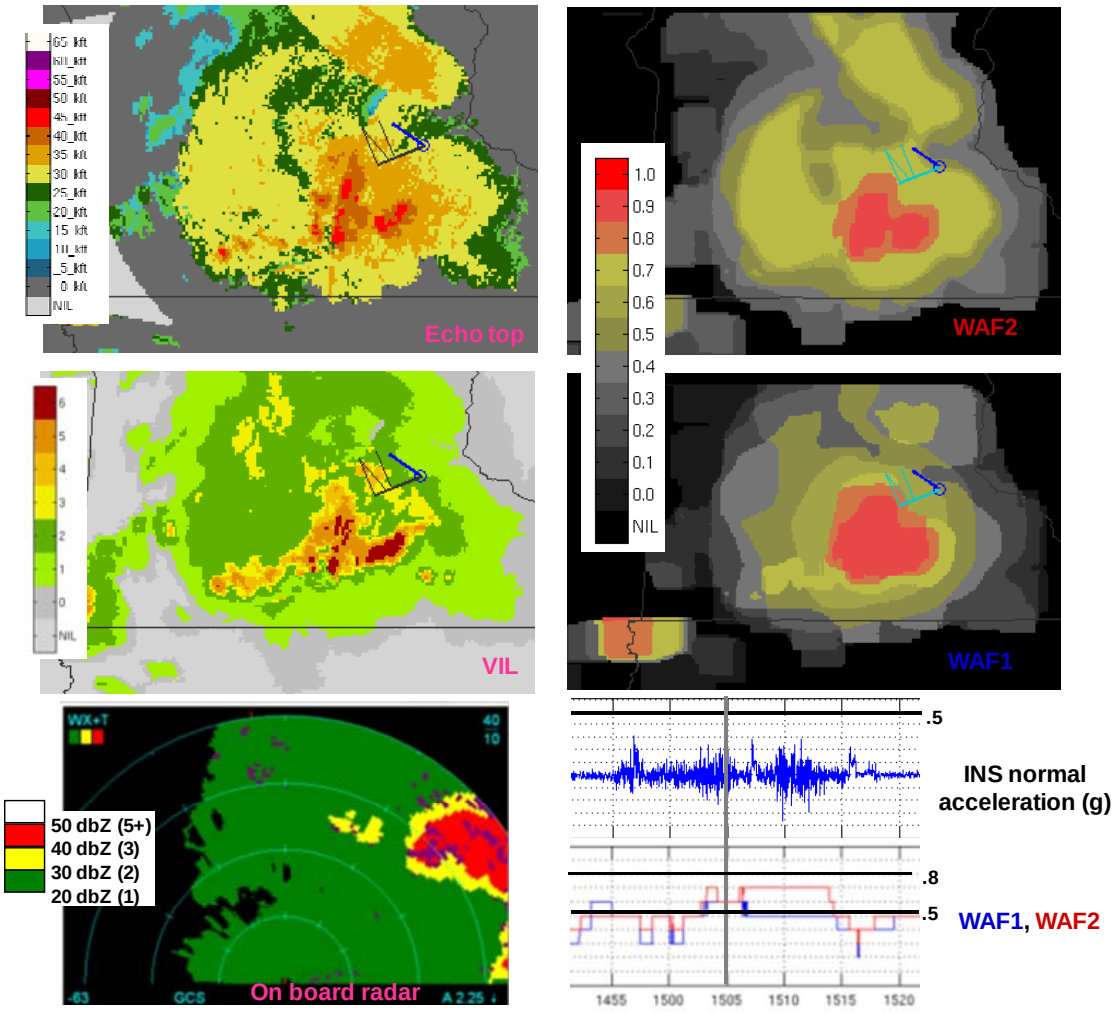

Figure 7. Entering turbulence downwind of a convective system for flight 1. Ground and radar data at 1515z.

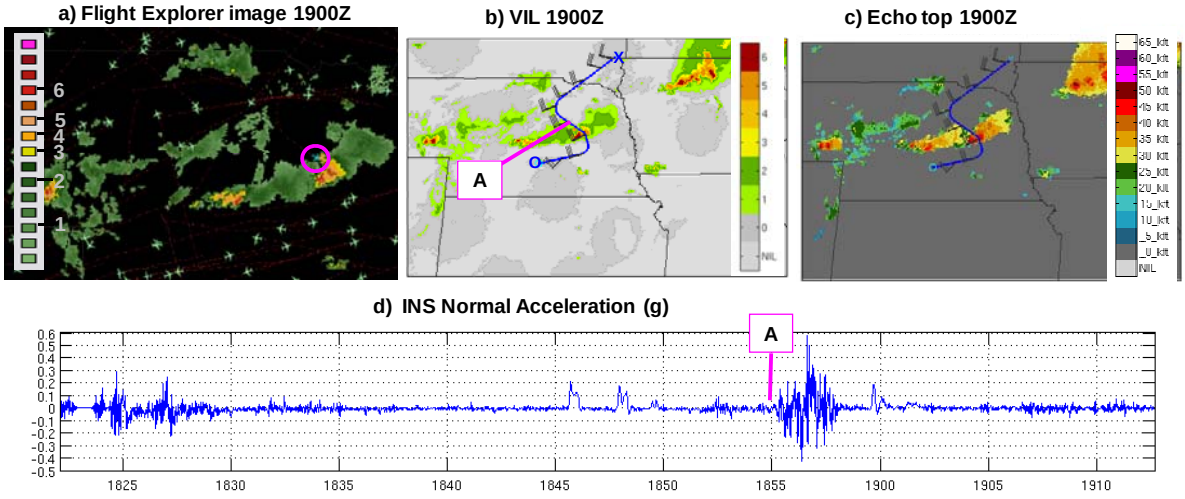

Figure 8. Same illustration as figure 5, for a selected portion of flight #2 on 17 July, 2008.

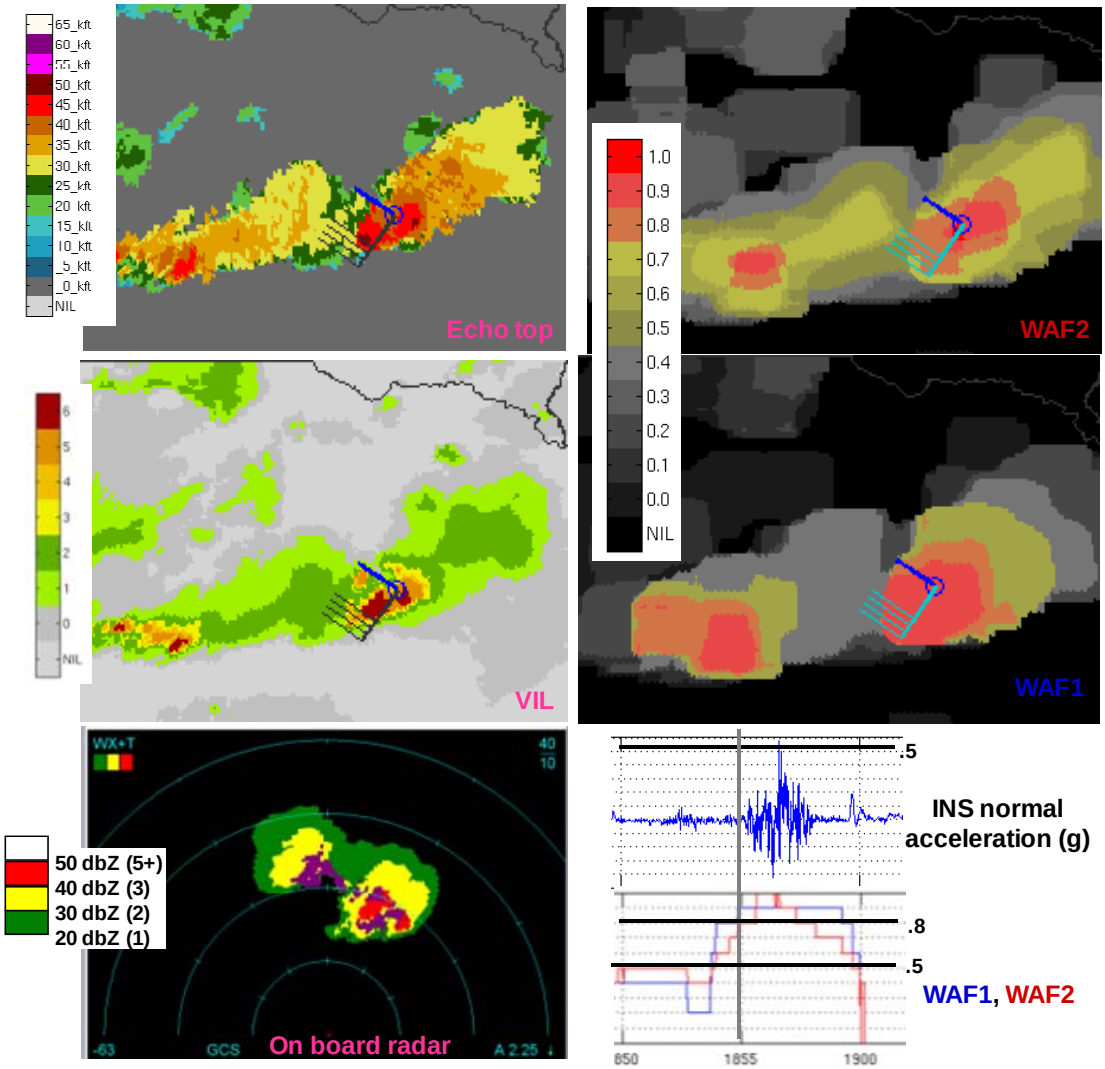

Figure 9. Encountering a vigorous convective core during flight 2. Ground and airborne radar data at 1900z.

The third and final flight of the day ran from approximately 2200Z – 2345Z and covered much of the same area as flight 2, but landed back at Cedar Rapids (figure 10). It flew longitudinally through a line of level 2-6, 50+kft convective cells. Commercial traffic generally avoided the line, staying well beyond the southern (leading) edge or to the north, far downwind from the most vigorous convection.

The aircraft first circled a small, intense cell, experiencing moderate turbulence (0.2 - 0.3 g) while flying through WAF ranging from 0.60 to 0.90 (figure 10, pointer A). Again, the WAF field provided a buffer around high-gradient edges. The aircraft then entered a line of several intense (level 6, 50kft) cells, experiencing moderate turbulence (0.2 - 0.3 g) and WAF probabilities between 0.70 and 1.0 (figure 10, pointer B). It continued to experience light to moderate turbulence as it emerged downwind, to the trailing edge of the line in level 2 VIL, 40kft echo tops (figure 10, pointer C and figure 11). Eventually, as the aircraft continued downwind, it entered a region of minimal turbulence, characterized by level 2 VIL and 40 kft echo tops. The winds here (10 – 30 knots) were lighter than those experienced during flight 1 (figure 10, pointer D). As in the first flight, there was good general agreement between on board and ground based radar, and the boundary between relatively calm and turbulent regions was not readily apparent from the radar data.

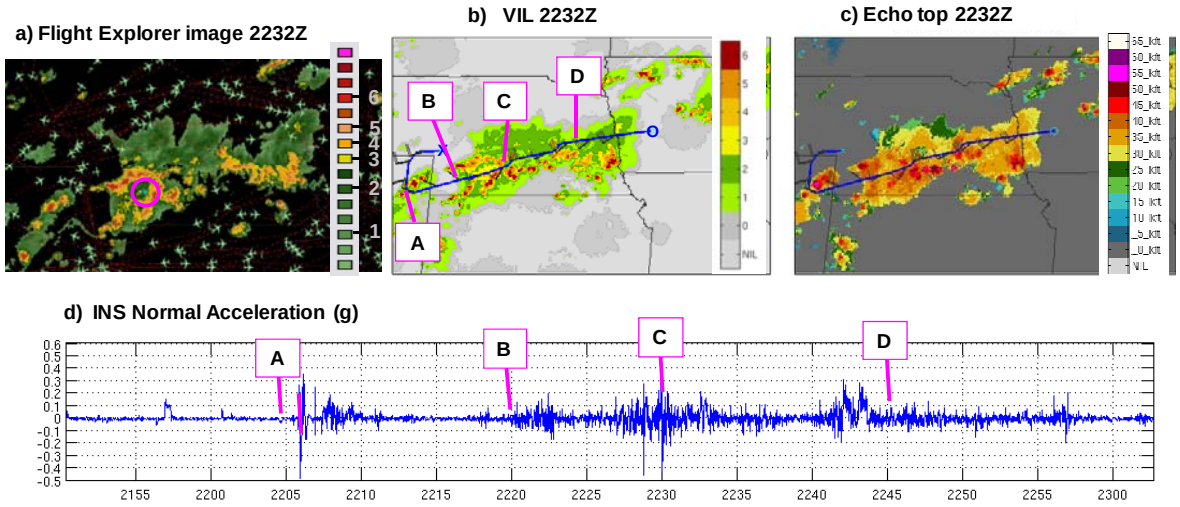

Figure 10. Same illustration as figure 5, for flight #3 on 17 July, 2008.

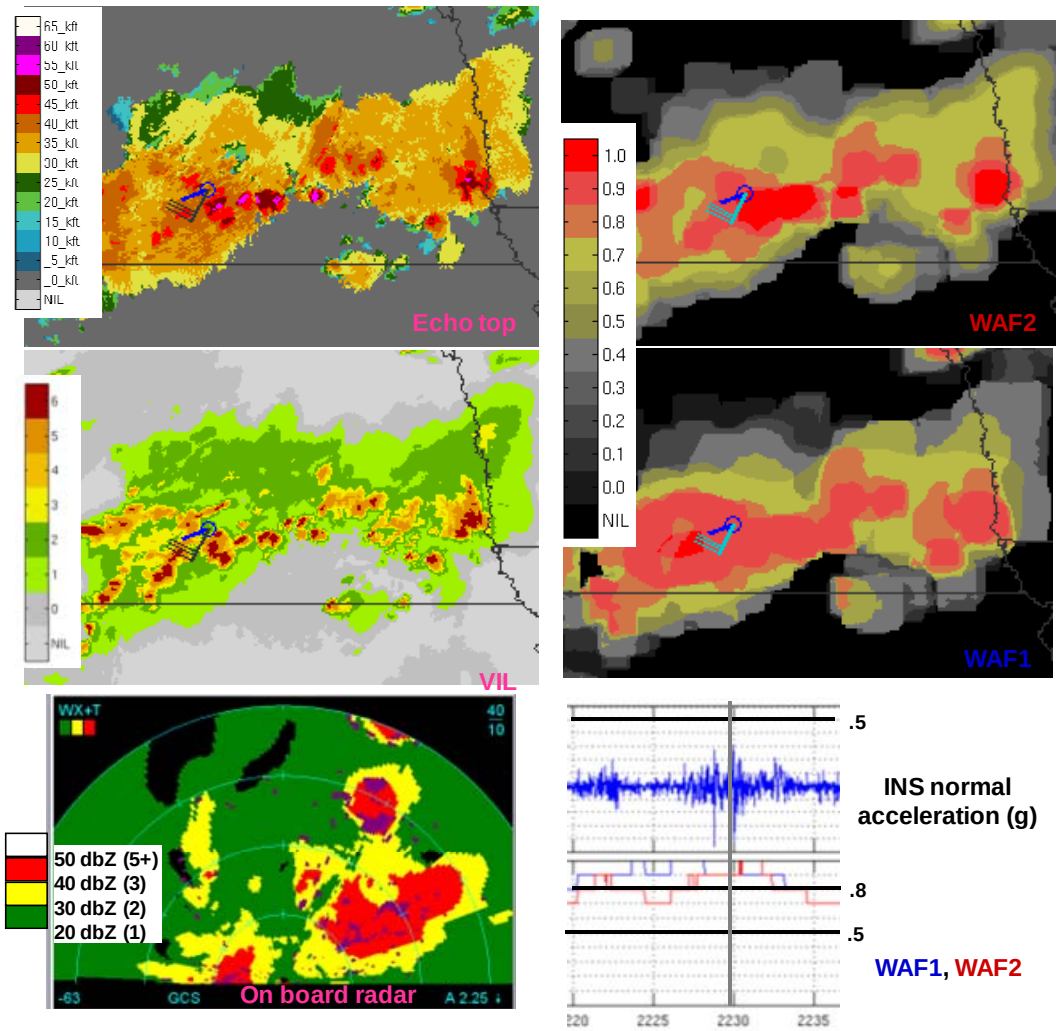

Figure 11. Flying through a complex of intense convective cells, encountering moderate turbulence during flight 3.

4.2 Day 2: 14 August, 2008

A 500mb trough axis existed between a cut-off low over the Northern Plains and a low pressure center north of New England. A surface trough was also establishing itself across the Missouri Valley. The atmosphere became sufficiently unstable during the heat of the afternoon to produce numerous showers and thunderstorms across Iowa and Minnesota.

A single mission was flown for the day from approximately 2000Z – 2245Z. Convection was present throughout southeast Minnesota and northeast Iowa.

Small, scattered 'popcorn' thunderstorms, characterized by VIL levels 5 – 6 and echo tops between 35 – 40kft were encountered during much of the route. Figure 12 shows the full flight trajectories and time series of normal acceleration for the flight. Note the presence of a small number of aircraft flying in the mission region. Nearby aircraft were mostly general aviation aircraft, flying at altitudes of 40kft or greater. Light to moderate turbulence was encountered at several points along the flight; WAF deviation probabilities ranged from 0.50 to 0.80 during these encounters. The scattered, disorganized convection of day 2 presents different challenges from the convection on day 1, which was characterized by larger, more vigorous cells (or complexes of cells), whose impacts were spread into sizeable downwind anvils by strong upper level winds. The individual cells on day two could be more easily avoided or even flown through, since the encounter with light to moderate turbulence was likely to be brief. In this sort of weather, the willingness of pilots to fly through a particular region of airspace may become a function of WAF, the density of cells and the ability to transit the airspace and avoid turbulent encounters, without excessive maneuvering. Analysis of day 2 data has been limited to date, but will be taken up as future work.

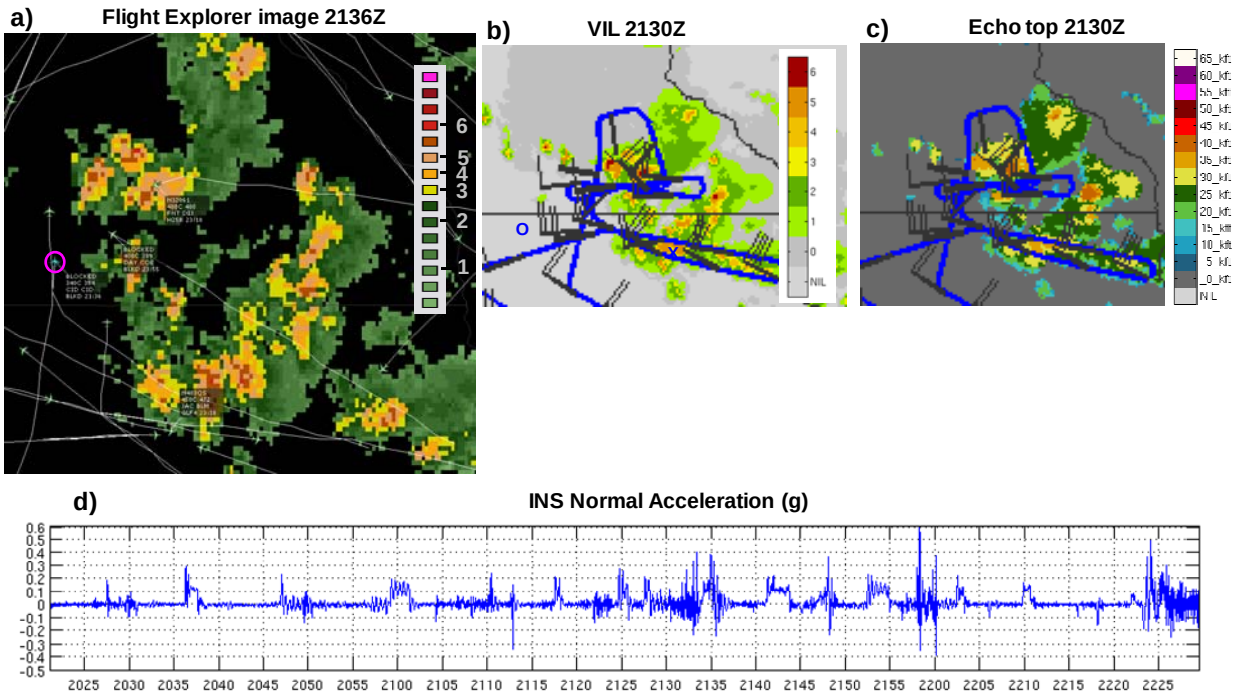

Figure 12. Summary of flight mission on 14 August, 2008.

5. DATA ANALYSIS AND RESULTS

5.1 WAF performance statistics

WAF deviation probabilities encountered along the research aircraft trajectory were compared to the normal accelerations recorded from the aircraft INS, in order to relate WAF to turbulence. Several isolated positive increases in the INS normal acceleration, to approximately 0.2 g, were associated with aircraft turns whose bank angles ranged between 15 and 28 degrees (measured by the INS roll angle). Smaller bank angles, usually less than six degrees, were associated with turbulence. Turns were removed from the comparison by editing out data where the bank angles were greater than 6 degrees and normal acceleration less than 0.2g.

Two statistical analyses of the relationship between measured turbulence and WAF deviation probabilities were performed. In the first analysis, the distribution of measured turbulence (none, light, moderate, heavy, severe) was calculate for each WAF deviation probability (0, 0.1, 0.2, etc.). Before the distributions were calculated, the data were downsampled from 50 Hz to 10 Hz, by taking every 5th sample, to reduce the computational time required to do the analysis. At a flight speed of 300 kts. (roughly the speed flown during the data gathering), a 10 Hz sample rate corresponds to a spatial sampling resolution of approximately 50 ft. (15 m.). The downsampled time series of the measured normal acceleration was run through a moving window filter that identified the local maximum of the absolute value of normal acceleration within a 5 second interval. The 5 second interval corresponds to approximately 2500 ft. (800 m.), slightly less than the spatial resolution of the WAF grid. The filtered data approximate the maximum acceleration encountered in each WAF pixel encountered by the flight. Figure 13 illustrates the results of this INS normal acceleration filter.

Histograms of the normalized distribution of peak measured turbulence as a function of WAF deviation probability are plotted in figure 14 for WAF from both CWAM 1 and CWAM 2. Moderate turbulence is encountered only in regions where WAF deviation probabilities exceed 0.70. The ratio of light to negligible turbulence also increases as the WAF deviation probability increases (except for an unexplained increase in light turbulence encounters at deviation probabilities of 0.10 and 0.20). A comparison between WAF from CWAM 1 and CWAM 2 suggests the larger WAF values from CWAM 2 agree slightly better with measured turbulence than WAF values from CWAM 1.

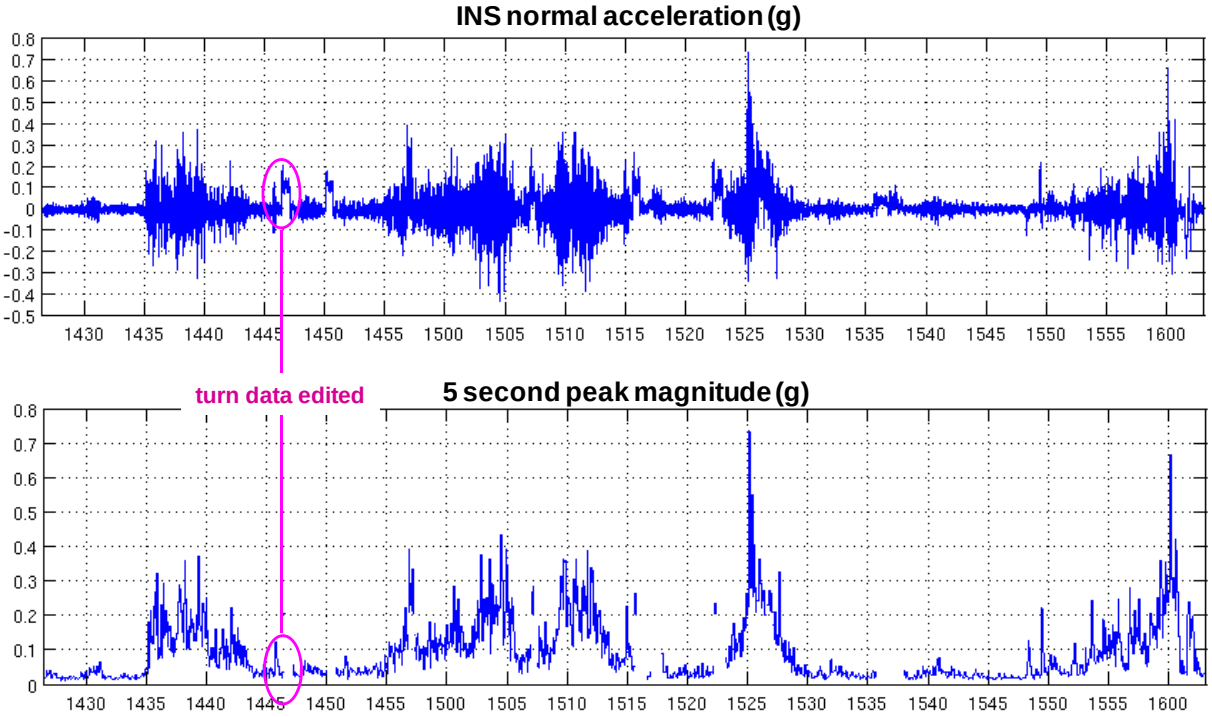

Figure 13. Time histories plot of INS normal acceleration (top) and filtered time histories showing local acceleration maxima, with turns removed (bottom). Data are from flight #1 of 17 July.

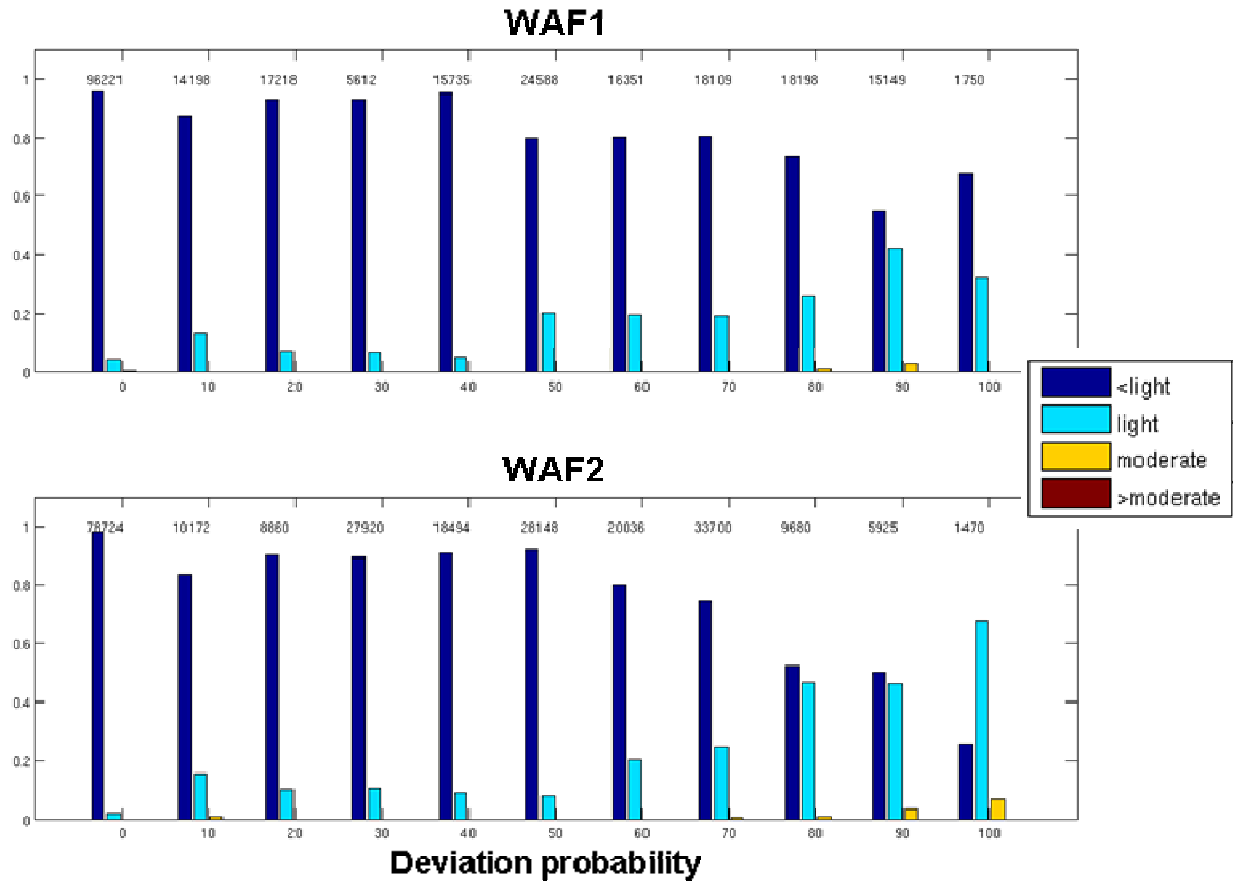

Figure 14. Histograms of normalized distribution of turbulence encountered, partitioned by WAF deviation probability. Top plot is for WAF from CWAM 1, bottom plot is for WAF from CWAM 2. Numbers above the histograms give the total number of data points in each WAF deviation probability partition.

Figure 15 presents an alternative statistical analysis. The magnitude of normal acceleration was calculated for turn-filtered, full 50 Hz INS data, and the range of the maximum and 90th percentile magnitude was calculated for each WAF deviation probability for both CWAM 1 and 2. Again, the comparison suggests that WAF from CWAM 2 better identified regions of turbulence. The greater tendency of CWAM 1 to assign higher WAF values to regions of light turbulence is likely related to the larger spatial filter applied to the VIL input, which results in larger WAF buffers around regions of high convective intensity. The difference between the 90th percentile and the maximum value encountered is attributed to the non homogeneous nature of the atmosphere. Equivalent WAF can result in different turbulent encounters. Intensity and echo tops may be a first order indication of turbulence. Given that pilots avoid low values of turbulence for ride considerations, a model such as CWAM 2 may be useful.

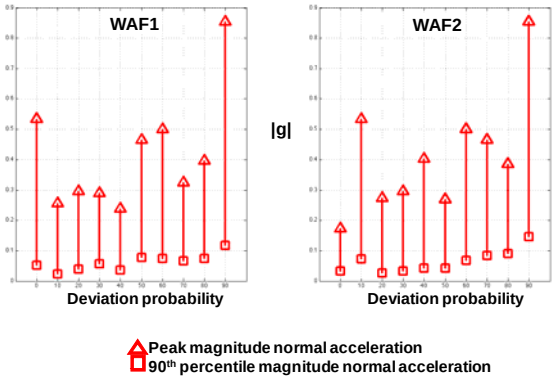

Figure 15. Range of maximum 10 percent of normal acceleration magnitudes as a function of WAF deviation probability from CWAM 1 and CWAM 2 for Flight Day 1.

A precise correlation between WAF deviation probability and normal acceleration is not expected, nor is it necessarily desirable, since the WAF deviation probability should take into account all of the factors that a pilot considers in making the decision to deviate, including the possibility of

encountering lightning, hail or graupel, in addition to the likelihood of turbulence. The WAF must also include spatial buffers needed to account for uncertainty about the precise location of convective hazard and pilot tolerance for the risks associated with convective weather encounters in en route airspace. Capturing accurately this 'sphere of convective influence' is an important aspect of both versions of the CWAM.

5.2 Qualitative results

From a detailed analysis of the normal acceleration and aircraft location for flights 1 and 3 of 17 July, it was possible to identify the entry and exit points of turbulent regions. By noting the relationship of these entry and exit points to storm features and prevailing winds, notional 'turbulence envelopes' were drawn. There turbulence envelopes, shown in figure 16, separate regions of moderate or greater turbulence near to and downwind from the most vigorous convective cells from the regions of minimal turbulence in decaying convection and stratiform rain. A similar analysis, based on the on board video, was used to identify the boundary between visual and IMC for flight 1.

Some of the area outside the turbulence envelopes – between the VMC (Visual Meteorological Conditions) and turbulence boundary in front of the storm, or in the high-topped stratiform region behind it – is airspace that is often avoided by commercial traffic. The data presented here suggest that some of this airspace may, in fact, be passable, albeit with some risk of encountering light to moderate turbulence. A WAF that can robustly differentiate regions with high likelihood of turbulence from those that are likely to be calm, with an operationally realistic buffer to account for uncertainty, could support a more consistent use of passable airspace that is currently avoided.

Unfortunately, the transition between turbulent and non-turbulent regions was not readily apparent from either the ground-based radar or the WAF derived from it. Since echo top height is the primary factor in WAF deviation probabilities in both models, deviation probabilities tended to be high in both regions of high-topped stratiform and downwind anvils. Deviation probabilities from the CWAM 1 WAF tended to be slightly lower in both regions, since level 1 and 2 VIL predominates and CWAM 1 WAF are functions of VIL level 3 coverage as well as echo top height. CWAM 2 WAF tended to have smaller buffers around vigorous convection, since the window used in the spatial filter that it applies to the radar data is smaller. WAF from both CWAM 1 and CWAM 2 also showed generally good agreement with the on board weather radar.

It is noteworthy that nothing more severe than moderate turbulence was experienced, even while flying through convective cells characterized by VIL levels 5-6 and 50+ kft echo tops. Heavier aircraft such as a typical commercial airliner would experience somewhat less severe turbulence than the Sabreliner. This is not to imply that pilots should routinely penetrate such cells! Rather, it suggests that several factors may play a part in observed pilot deviation behavior. The expectation of moderate or even light turbulence may be an appropriate rule of thumb to determine the threshold for deviation.

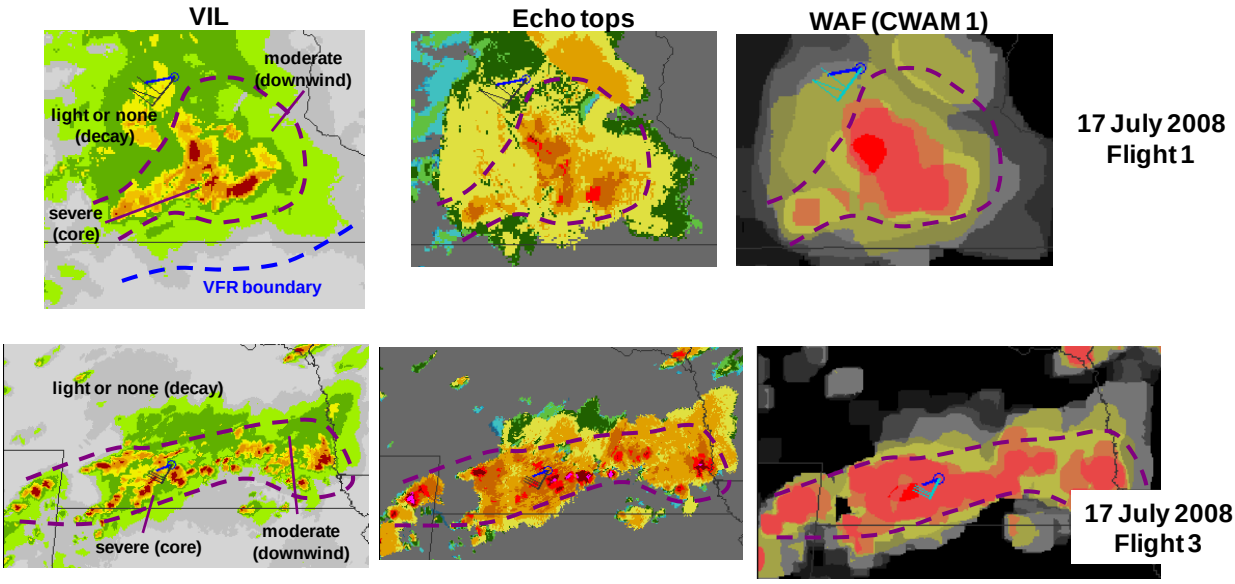

Figure 16. Notional 'turbulence envelopes' around convective storm complexes.

6. CONCLUSIONS

Four flight missions, flown by an instrumented Rockwell Sabreliner Model 50 research aircraft on two different days in the upper Midwest, gathered data from several regions of interest in and around strong convection. INS acceleration and wind data, along with cockpit audio, video, photos and on-board weather radar images, were taken from the aircraft. The aircraft was operated within and around convective storms where few commercial aircraft were observed. Data were gathered from several areas of the storms, including the convective core, leading (growing) edge, downwind anvil, decaying convection and nearby stratiform rain associated with mesoscale convective complexes, and from a region of scattered thunderstorms.

The measured aircraft normal accelerations were compared with the WAF derived from ground-based radar to evaluate its ability to identify regions of significant turbulence. Comparisons were made for the WAF calculated using two different Convective Weather Avoidance Models (CWAM 1 and 2). While it is important not to overestimate the generality of the results from a few hours of data gathered from four flights, the data provide useful insights into the factors that may affect pilots' decisions about when to deviate to avoid convective weather.

Regions of moderate turbulence in and around convective cores were characterized by high WAF deviation probabilities, ranging from 0.70 to 1.0 (70% to 100%). The ratio of light turbulence encounters to no turbulence correlated well with WAF deviation probabilities, as did the range between the 90th percentile and maximum normal acceleration measurements. WAF calculated using CWAM 2 appeared to correlate somewhat better with observed turbulence than those calculated using CWAM 1.

In many instances, high deviation probability contours in the WAF extended beyond the bounds of the highest turbulence, rapidly decreasing as one moved farther from the convective core into clear air (buffers in CWAM 1 WAF tended to be larger than those in CWAM 2 WAF). In these cases, some additional WAF buffer around the active storm is probably desirable, since pilots are unlikely to fly right along storm boundaries even in visual meteorological conditions, when they have a clear view of the storm. The challenge is to determine a buffer size that accounts for uncertainty and pilot comfort, while not closing down airspace that may be safely passable.

Neither WAF could discriminate well between non-turbulent high-topped stratiform rain and downwind anvils, since both regions were characterized by similar VIL and echo top signatures. In both regions, WAF deviation probabilities ranged roughly from 0.40 to 0.80. Using upper level winds and weather fields or WAF that clearly identify strong convection, it may be possible to differentiate downwind regions that are likely to be turbulent from non-turbulent stratiform rain. The challenges in this approach are to identify the convective regions that can induce downwind turbulence and to estimate how far downwind one must go to escape the turbulence.

Visual feedback from the cockpit also suggested that radar reflectivity alone is insufficient to differentiate between regions of VMC and IMC flight. This is despite reflectivity features that were observed from the on board weather radar display and generally showed good agreement with both ground-based radar products and WAF. A partition between VMC and IMC regions, based on some combination of radar, satellite and model data, may be a useful input to CWAM. Visual cues, when they are available, are likely the most important factor in pilot decision making. Recognizing when and where pilots can maintain VMC flying while avoiding convective weather is likely to increase the robustness of automated algorithms that create weather-avoiding reroutes.

The primary focus of this study was to compare the WAF with quantitative measurements of normal accelerations. However, it is important to recognize that the WAF is intended to predict pilot behavior, not the likelihood of turbulence encounters. Other factors that influence the pilot's decision to avoid convective weather, such as the possibility of encountering hail or lightning, or the differences in risk tolerance among pilots, must also be accounted for in the WAF. It is recognized that the other data collected in this study are comprehensive enough to be used to gather more information about additional factors in pilot decision-making and is recommended as future work.

7. FUTURE WORK

Since the decision to deviate rests ultimately with the pilot, further research into human factors is needed to ensure that CWAM capture the critical elements of pilot decision making. It is important that automatically generated weather-avoiding reroutes be acceptable to pilots. Pilots must be confident that the WAF partitions the airspace accurately into passable and impassable regions. To date, human factors research has been based either on small sample, focus group studies (O'Hare et. al., 1995; Mosier et. al., 1998, for example) or statistical studies (DeLaura and Evans, 2006; DeLaura et. al., 2008; Kuhn, 2008) that require potentially error-prone inferences about pilot behavior and intent. What is needed is a way to take data from studies that capture many details of the flight experience (ground-based radar, cockpit radar, visual cues, turbulence encountered, etc.) and package them in a way that can be widely distributed to pilots in an effort to gather data about the specific factors that influence their decision in convective weather. The presentation of the data must be sufficiently true to operational experience that pilots are able to make accurate judgments of their behavior in conditions similar to those presented. How to accomplish this is left as a challenge to researchers in the field!

Other work could extend the WAF generation beyond the tactical domain supported by CIWS. With the development of longer range forecasts such as the Consolidate Storm Prediction for Aviation (CoSPA) (Dupree, et. al., 2009), longer range WAF predictions may be applied to automated decision support in the strategic (2 – 8 hour) time frame as well assuming the necessary information are available.

Additionally, in-situ turbulence measurements (Cornman, et. al., 2004) and model-based estimates of convectively induced turbulence (Williams, et. al., 2006) may provide additional information that could help discriminate between high-topped stratiform rain and downwind turbulent anvils. The authors of this study plan to consider both data sources in a follow-up study

7. ACKNOWLEDGMENTS

The authors wish to acknowledge the mission team from Rockwell Collins for their skill and valuable insights into the operational usage and interpretation of cockpit instrumentation:

Pilots: Barry A. Brown, John J. Kelchen, Jr., Thomas E. Yerke
Engineers: Roy Robertson, Greg Koenigs

8. REFERENCES

Chan, William, Mohamad Refai, Rich DeLaura: "Validation of a Model to Predict Pilot Penetrations of Convective Weather", 7th AIAA Conference on Aviation, Technology, Integration and Operations, Belfast, Ireland, September, 2007.

Cornman, L. B., G. Meymaris, M. Limber: "An Update on the FAA Weather Research Program's *in situ* Turbulence Measurement and Reporting System", 11th Conference on Aviation, Range and Aerospace Meteorology, American Meteorological Society, Hyannis, MA, January, 2004.

DeLaura, Rich, James Evans: "An Exploratory Study of Modeling Enroute Pilot Convective Storm Flight Deviation Behavior", 12th Conference on Aviation, Range and Aerospace Meteorology, American Meteorological Society, Atlanta, GA, Jan., 2006.

DeLaura, Rich, Mike Robinson, Margo Pawlak, Jim Evans: "Modeling Convective Weather Avoidance in Enroute Airspace", 13th Conference on Aviation, Range and Aerospace Meteorology, American Meteorological Society, New Orleans, LA, Jan., 2008.

Dupree, W., D. Morse, M. Chan, X. Tao, C. Reiche, H. Iskenderian, M. Wolfson, J. Pinto, J. Williams, D. Albo, S. Dettling, M. Steiner, S. Benjamin, S. Weygandt: "The 0-6 Hour Consolidated Storm Prediction for Aviation (CoSPA) Forecast Demonstration 2008"**,** Aviation, Range and Aerospace Meteorology Special Symposium on Weather – Air Traffic Management Integration, Phoenix, AZ, Jan. 2009.

FAA REDAC, 2007, "Weather-Air Traffic Management Integration Final Report," Weather – ATM Integration Working Group (WAIWG) of the National Airspace System Operations Subcommittee, Federal Aviation Administration (FAA) Research, Engineering and Development Advisory Committee (REDAC)., 3 October 2007 (to be available at http://research.faa.gov/redac/)

Klingle-Wilson, D., J. Evans: "Description of the Corridor Integrated Weather System (CIWS) Weather Products", MIT Lincoln Laboratory Project Report ATC-317, August, 2005.

Kuhn, Kenneth: "Analysis of Thunderstorm Effects on Aggregated Aircraft Trajectories", Journal of Aerospace Computing, Information and Communication, Vol. 5, April, 2008.

Lester, P. F., 1993: Turbulence. Jeppesen Sanderson Inc., Englewood, Colorado, 275 pp.

O'Hare, David and Tracy Smitherham: "'Pressing On' Into Deteriorating Conditions: An Application of Behavioral Decision Theory to Pilot Decision Making", The International Journal of Aviation Psychology (1995), 5:4, pp. 351 - 370.

Mosier, Kathleen L., Linda J. Skitka, Susan Heers, Mark Burdick: "Automation Bias: Decision Making and Performance in High-Tech Cockpits", The International Journal of Aviation Psychology (1998), 8:1, pp. 47 – 63.

Williams, John K., Larry B. Cornman, Jaimi Yee, Steven G. Carson, Gary Blackburn, Jason Graig: "NEXRAD Detection of Hazardous Turbulence", 44th American Institute of Aeronautics and Astronautics Science Meeting and Exhibits, Reno, NV, January, 2006.

World Meteorological Organization, 1998: Manual on Codes, *Vol. I, WMO – No. 306*, I-D-16. 1998.